World Journal of Engineering Research
Print ISSN: 2959-9865
Online ISSN: 2959-9873
DOI: https://doi.org/10.61784/wjer3108

CNN-GRU-BASED DEFORMATION PREDICTION METHOD FOR SUBWAY EXCAVATIONS

ChenShu Meng[1], Hui Wang[1*], YanHui Zhang[2], ZiJie Li[1], Yu Sun[1]
[1]*Hebei GEO University, Shijiazhuang 052161, Hebei, China.*
[2]*China Mobile Communications Group Hebei Co., Ltd., Shijiazhuang 052161, Hebei, China.*
[*]*Corresponding Author: Hui Wang*

Abstract: To address the issues of decreased deformation prediction accuracy and early warning lag caused by missing monitoring data during subway foundation pit construction, this paper proposes a deformation prediction method based on the CNN-GRU neural network. First, a convolutional neural network (CNN) is used to impute missing data in the original monitoring sequence. Second, wavelet decomposition is applied to decompose the imputed sequence into a trend component and a noise component. Third, a gated recurrent unit (GRU) neural network is constructed to predict the trend component, while an ARMA model is used to fit and predict the noise component. Finally, the prediction results of the two parts are reconstructed to obtain the final deformation prediction value. This paper conducts an empirical analysis using the vertical displacement monitoring data of the wall top of No. 2 air vent at Terminal 3 Station of B Airport. The results show that with a missing rate of 5.8%, the proposed model achieves a mean absolute percentage error (MAPE) of 1.93% and a coefficient of determination (R^2) of 0.95. Compared with GA-BP, LSTM, single GRU, and ARMA models, all error metrics are significantly reduced, and the prediction lag problem is effectively improved. This method provides an effective solution for deformation prediction of foundation pits under incomplete data conditions.
Keywords: Foundation pit; Deformation prediction; CNN; GRU

1 INTRODUCTION

With the acceleration of urbanization in China, urban rail transit construction has entered a period of rapid development. As key engineering nodes, deep foundation pits of subway stations are characterized by large excavation depths and complex surrounding environments, and their construction safety directly determines the success or failure of the project[1]. Deformation monitoring of foundation pits is an important means of ensuring safety. By obtaining real-time data such as wall top settlement and diaphragm wall horizontal displacement, anomalies can be detected promptly and control measures can be implemented. However, in actual monitoring, data loss often occurs due to sensor failure, signal interference, transmission interruption, and other reasons, which disrupts the continuity of the time series, leading to reduced accuracy of deformation prediction and delayed early warning, thereby posing risks to construction safety[2]. In recent years, traditional prediction methods such as time series analysis, grey models, and BP neural networks have performed well when data are complete, but they are sensitive to missing data. Common interpolation methods struggle to capture the nonlinear characteristics of deformation, and interpolation errors tend to accumulate and amplify with prediction. Therefore, achieving high-precision deformation prediction under data-missing conditions has become an urgent problem to be solved in the field of foundation pit monitoring. To address the above shortcomings, this paper proposes a CNN-GRU hybrid model that uses CNN to impute missing data and GRU to perform deformation prediction. The effectiveness of the method is verified using the vertical displacement monitoring data of the wall top of No. 2 air vent at Terminal 3 Station of B Airport.

2 RELATED RESEARCH METHODS

2.1 CNN

Convolutional Neural Networks(CNN)are a class of feedforward neural networks that employ convolution operations and possess deep structures. Through the combination of convolutional layers, pooling layers, and fully connected layers, this type of network can automatically extract local features from input data, and on this basis, compress information layer by layer to remove redundancy, thereby enhancing the model's generalization ability[3]. Due to the design of parameter sharing and local connectivity, CNNs achieve high efficiency when processing grid-like data and typically do not rely on additional feature engineering. Their core structure is shown in Figure 1.
The convolutional layer performs convolution operations between convolution kernels and the input data to extract local features of the data. The convolution kernel slides over the input data, covering a local region each time, and obtains the feature value at that position through weighted summation. Through the parallel operation of multiple convolution kernels, the CNN can extract multi-dimensional and multi-scale feature information from the raw data. This process can be expressed by the following formula:

$$y_j=f\left(\sum_{i=1}^{k} w_i \cdot x_{j+i-1}+b\right) \quad (1)$$

The pooling layer usually follows the convolutional layer. Its function is to reduce the dimensionality of the features output by the convolutional layer, thereby decreasing computational parameters while retaining the main features. The pooling operation not only reduces the feature dimensionality but also enhances the model's robustness to small shifts in the input data.

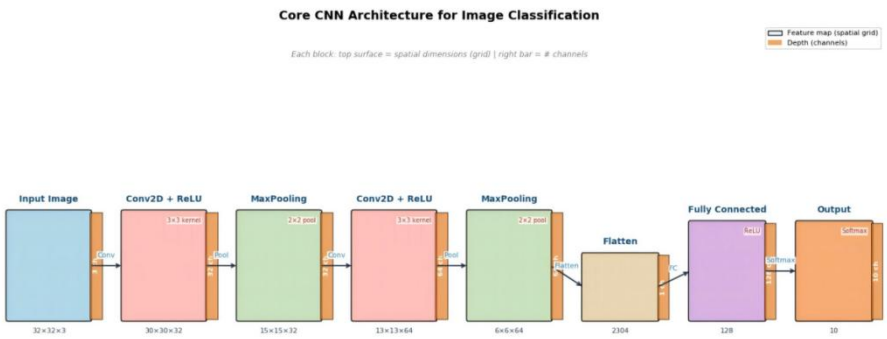

Figure 1 Core CNN Architecture for Image Classfication

The fully connected layer globally integrates the local features extracted by the convolutional and pooling layers, and then maps the distributed feature representations to the sample label space, thereby completing classification or regression tasks.

In this paper, CNN is applied to impute missing values in time series[2]. Based on the observations in the neighborhood before and after a missing point, the convolutional operation is used to learn local temporal patterns and thereby predict the missing value. A fixed-length time window centered on the missing point is extracted as input, with the known observations within the window serving as features and the missing position as the target to be predicted. A CNN is then constructed to fit the mapping relationship between the data within the window and the missing value.

2.2 GRU

GRU is an improved form of RNN. Traditional RNNs are prone to the vanishing gradient or exploding gradient problem when processing long sequences. GRU addresses this issue while simplifying the complex structure of Long Short-Term Memory (LSTM) networks, reducing computational parameters and improving model training efficiency while maintaining comparable performance[2,4]. However, when the sequence is long, the gradient needs to be multiplied over multiple time steps during backpropagation, which leads to exponential decay or growth of the gradient, making it difficult for the model to learn long-distance dependencies. Its core structure is shown in Figure 2.

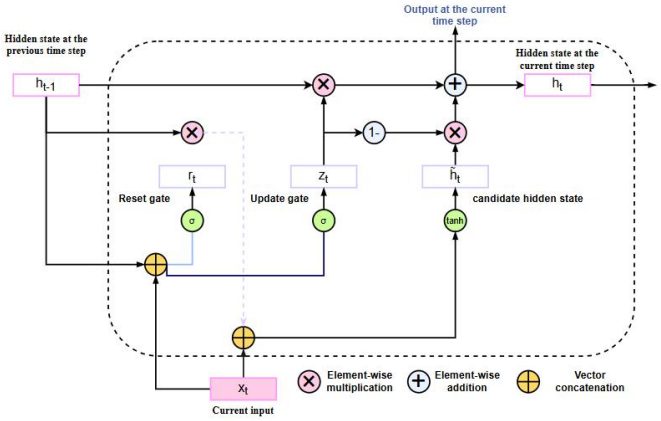

Figure 2 Core structure diagram of GRU

Traditional RNN passes the hidden state from the previous time step to the current time step through recurrent connections, theoretically enabling it to capture historical information in time series. Its basic calculation formula is:

$$h_t = \tanh\left(W \cdot [h_{t-1}, x_t] + b\right) \quad (2)$$

LSTM effectively alleviates the vanishing gradient problem by introducing three gating mechanisms—input gate, forget gate, and output gate—along with a memory cell, making it a mainstream model for processing long sequences. However, LSTM has a relatively complex structure, many parameters, and a long training time. GRU simplifies LSTM by merging the forget gate and input gate into an update gate, and combining the memory cell with the hidden state, retaining only two gating units: the update gate and the reset gate. This design gives GRU fewer parameters and a more concise structure, allowing it to achieve performance comparable to LSTM in most tasks while enabling faster training[5]. Its forward propagation process is described by the following formulas:

The reset gate controls the extent to which the previous hidden state influences the current candidate hidden state:

$$r_t=\sigma\left(W_r\cdot\ [h_{t-1},x_t]+b_r\right) \tag{3}$$

The update gate controls the proportion of the previous hidden state that is retained into the current hidden state:

$$z_t=\sigma\left(W_z\cdot\ [h_{t-1},x_t]+b_z\right) \tag{4}$$

The candidate hidden state combines the current input with the historical information adjusted by the reset gate:

$$\tilde{h}_t=\tanh\left(W_h\cdot\ [r_t\odot h_{t-1},x_t]+b_h\right) \tag{5}$$

The current hidden state performs a weighted fusion of the previous hidden state and the candidate hidden state via the update gate:

$$h_t=(1-z_t)\odot h_{t-1}+z_t\odot\tilde{h}_t \tag{6}$$

From the above formulas, the working mechanism of GRU can be observed:

When the reset gate is close to 0,the model ignores historical information and generates the candidate state solely based on the current input, which helps capture short-term dependencies.When the update gate is close to 1, the model retains more of the historical state while the current input has less influence, which helps capture long-term dependencies. Through the balance between and 1-z_t,the GRU can adaptively determine the fusion ratio of historical information and current information.

2.3 Wavelet Decomposition

Wavelet decomposition is a signal processing technique that can decompose a signal according to different frequency scales. Deformation monitoring data of subway foundation pits contain both low-frequency components reflecting the overall trend and high-frequency random fluctuations caused by factors such as construction disturbances and measurement errors. Wavelet decomposition can separate the original sequence into a low-frequency trend component and a high-frequency noise component, providing a basis for subsequent separate modeling.

For discrete time series, the discrete wavelet transform achieves fast decomposition through the Mallat algorithm. Let the original signal be S,After one-level decomposition, the approximation component A_1 (low-frequency) and the detail component D_1 (high-frequency).The approximation component is then further decomposed. After n -level decomposition, the original signal can be expressed as the sum of the components at each level:

$$S=A_n+D_1+D_2+\cdots\ +D_n \tag{7}$$

The choice of wavelet basis affects the decomposition performance. In this study, the sym8 wavelet basis is adopted, which has good regularity and compact support, making it suitable for the analysis of foundation pit deformation data. The number of decomposition levels is determined according to the signal length. In this paper, a 3- level decomposition is performed, where the detail components are combined into the noise term $N=D_1+D_2+D_3$， and the trend term is retained as $T=A_3$.

2.4 ARMA Model

ARMAis a classical method for analyzing stationary time series and is often used to describe linear processes driven jointly by a series' own past values and random disturbances[6-7]. For a stationary time series $\{y_t\}$,the general form of the ARMA（p,q）model is:

$$y_t=c+\phi_1 y_{t-1}+\cdots\ +\phi_p y_{t-p}+\varepsilon_t+\theta_1\varepsilon_{t-1}+\cdots\ +\theta_q\varepsilon_{t-q} \tag{8}$$

2.5 Construction of CNN-GRU-Based Deformation Prediction Method for Subway Excavations

This method mainly consists of four core stages. The first stage is data preprocessing. First, the 3σ criterion is used to identify and remove outliers: if a data point falls outside the range $[\mu-3\sigma,\mu+3\sigma][\mu-3\sigma,\mu+3\sigma]$, it is considered an outlier and replaced by linear interpolation of the observed values at adjacent time points. Next, the Akima interpolation method is applied to convert the non- equally spaced monitoring data into an equally spaced time series. Finally, Min- Max normalization is used to map the data to the [0,1] interval, eliminating the effect of different units. Its expression is as follows:

$$x_{norm}=\frac{x-x_{min}}{x_{max}-x_{min}} \tag{9}$$

The second stage is the CNN missing data imputation phase, where a convolutional neural network is used to impute missing values[2]. A time window centered at each missing point is extracted, with the known values within the window serving as input features. A mask vector is added to indicate the positions of known values. A CNN learns the mapping from neighborhood observations to the missing value. The CNN network employs two one- dimensional convolutional layers to extract local features, followed by global average pooling and a fully connected layer to output the imputed value. The loss function is the mean squared error (MSE), and the optimizer is Adam. After training, all missing positions in the sequence are imputed to obtain the complete sequence $Y_{repaired}$。

Third, discrete wavelet decomposition is performed on the imputed complete sequence $Y_{repaired}$[8-9].The sym8 wavelet basis is selected with the number of decomposition levels n=3, yielding:

$$Y_{repaired}=A_3+D_1+D_2+D_3 \tag{10}$$

The detail components are combined into $N=D_1+D_2+D_3$， and the trend component is retained separately as $T=A_3$.The trend component reflects the main evolution law of the deformation, while the noise component reflects the random

fluctuation component.

Finally, the combined prediction and reconstruction stage is carried out. First, trend prediction is performed: a GRU neural network is used to model the trend component T. A multi-step rolling approach is adopted to construct samples. The GRU network employs a two-layer stacked structure, with dropout added between layers to prevent overfitting, and the output layer is a fully connected layer. After training, the trend component prediction value $\hat{T}$ is obtained. Next, noise prediction is performed: an ARMA model is used to fit the noise component N [6-7]. First, the ADF test is conducted to verify stationarity; then, the optimal (p,q) are determined using ACF/PACF plots combined with the AIC criterion. Maximum likelihood estimation is used to estimate parameters and test the validity of the model. The model is used for recursive prediction to obtain the noise component prediction value $\hat{N}$. Finally, the two prediction values are summed to obtain the final deformation prediction value $\hat{Y}$. RMSE, MAE, MAPE, and R2 are used to evaluate prediction accuracy, and the cross-correlation coefficient is used to analyze prediction lag.

The overall framework of the CNN-GRU deformation prediction method proposed in this paper is shown in Figure 3.

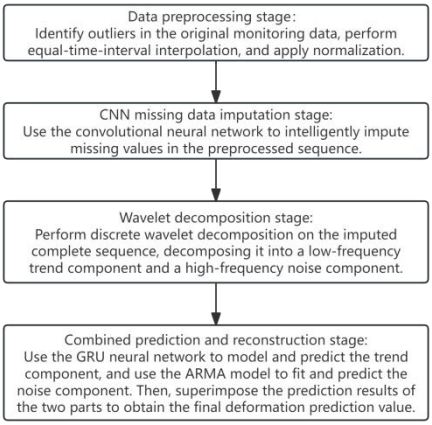

Figure 3 Overall Framework Diagram of the CNN-GRU Deformation Prediction Method

3 CASE VERIFICATION

3.1 Project Overview

The B Airport to G Station project [Terminal 3 Station of B Airport] has a station length of 315.8 m. It is a two-story underground frame structure with an island platform. The standard cross-section width of the station is 23.5 m. Terminal 3 Station of the airport is equipped with three groups of air vents, three entrances/exits, and two emergency exits. Among these, Emergency Exit No.1 is integrated with the main structure by a top-out arrangement. Air vent groups 1 and 3 are combined, while Entrance/Exit C and Emergency Exit No.2 are combined with Air Vent Group 2. The foundation pit of Air Vent Group 2 is taken as the research object of this paper. The pit has plan dimensions of approximately 20.65 m*20.0 m and an excavation depth of about 10.1 m. The cut-and-cover method is used for construction. The retaining structure consists of 800 mm thick diaphragm walls combined with an internal support system, as shown in Figure 4.

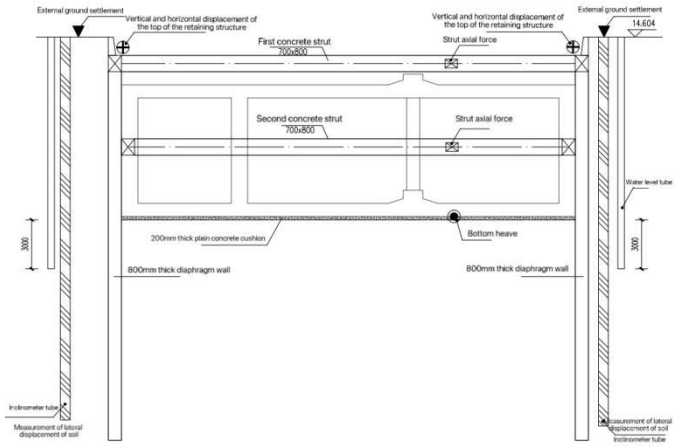

Figure 4 Monitoring Profile of the Auxiliary Foundation Pit of Terminal 3 Station of B Airport

According to the engineering survey data, the site stratigraphy from top to bottom consists of artificial fill, alluvial sand layers (silty sand, fine sand, medium sand, coarse sand), muddy soft soil layers, and Carboniferous strongly to weakly

weathered rock layers. Among them, shallow soft soil layers such as silt and muddy soil are distributed, characterized by low strength and high compressibility; the middle part contains saturated sand layers with high permeability. Within the excavation range of the foundation pit, the artificial fill, soft soil layers, and sand layers have poor mechanical properties, which can easily cause deformation of the retaining structure and instability of the foundation pit slope. In terms of hydrogeology, the groundwater types at the site include Quaternary pore water, bedrock fissure water, and karst water, with a water table depth of 3.40~8.60 m. The groundwater is recharged by atmospheric precipitation, with an annual variation range of approximately 2.5~3.5 m. The complex geological and hydrological conditions impose high requirements on the safety of foundation pit construction, and conducting high-precision deformation prediction is of great engineering significance[1,10].

Foundation pit monitoring was carried out in accordance with the *Technical Standard for Monitoring of Building Foundation Pit Engineering* (GB50497-2019) and relevant design documents. A total of monitoring points were arranged, including: 16 points for vertical displacement of the wall top, 16 points for horizontal displacement of the wall top, 7 points for inclinometer readings of the wall, 4 groups for support axial force, 19 points for ground surface settlement, and 8 points for groundwater level. The monitoring instruments used were a Leica DNA03 electronic level (accuracy ±0.3 mm/km), a TS11 total station (angular accuracy ±1), and an HCX-5 inclinometer (accuracy ±4 mm/15 m). All instruments were verified and certified as qualified. The monitoring frequency was dynamically adjusted according to the construction conditions: during excavation of the foundation pit, monitoring was performed once every 1~2 days; after the base slab was poured, the frequency was gradually reduced to once every 7 days.

In this paper, the vertical displacement monitoring point QCJ2-4 on the wall top is selected as a typical measuring point for modeling analysis. This point is located in the middle of the long side of the foundation pit of Air Vent Group 2. The measuring point uses a Φ14 mm stainless steel marker, welded to the main reinforcement of the capping beam, and the ground surface is protected by concrete encasement. The monitoring data span from September 28, 2021 to August 12, 2022, covering the entire construction process including foundation pit excavation, base slab pouring, structural backfilling, and subsequent deformation convergence. The sampling interval is mainly 2 days. A total of approximately 160 valid monitoring records were obtained, among which 7 data points are missing due to recording omissions and other reasons, giving a missing data rate of about 5.8%. The cumulative settlement variation pattern of this measuring point is clear and can well reflect the deformation characteristics of the retaining structure during construction, making it suitable for validation and comparative analysis of the deformation prediction model.

3.2 Data Preprocessing and Missing Data Repair

In this paper, the vertical displacement monitoring point QCJ2-4 on the wall top is selected as a typical measuring point. The monitoring period is from September 28, 2021 to August 12, 2022. The sampling interval is initially once every 2 days, and later gradually changes to 1 day, 3 days, 5 days, and 7 days, resulting in a non-equally spaced time series. In the original data of monitoring point QCJ2-4, there are 7 missing points due to recording omissions and other reasons, with a missing data rate of approximately 5.8%.

Taking the vertical displacement data of wall top at QCJ2-4 as the dependent variable, and the support axial force and groundwater level data as independent variables. To impute the missing displacement data for subsequent prediction, the cumulative settlement data of monitoring point QCJ2-4 on the wall top are used as the dependent variable samples of the model, and the nearby support axial force and groundwater level monitoring data are used as the independent variable samples of the model, together forming the missing data set. The missing data set consists of two parts: the missing data sample set and the complete data sample set.

To address the missing values in the original data of monitoring point QCJ2-4, this paper uses a CNN to impute the missing data. Known observations within the neighborhood window before and after the missing point are used as inputs, and the CNN learns local temporal features to estimate the deformation value at the missing position, thereby restoring the completeness of the monitoring sequence. The result of the missing data imputation is shown in Figure 5.

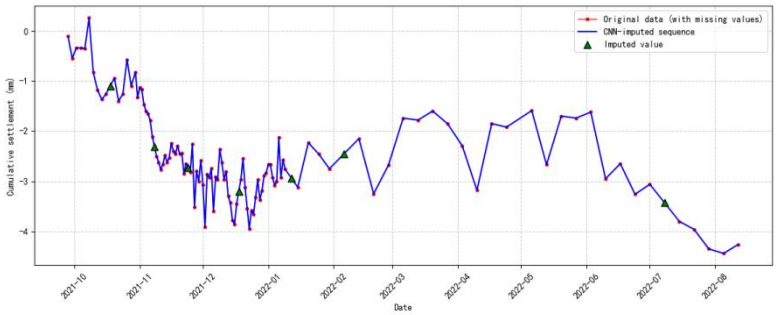

Figure 5 Comparison Chart of Missing Data Imputation for Monitoring Point QCJ2-4

3.3 Wavelet Decomposition and Component Extraction

Discrete wavelet decomposition is performed on the imputed complete sequence $Y_{repaired}$ [10-11].The sym8 wavelet basis is selected with the number of decomposition levels n=3, yielding:

$$Y_{repaired}=A_3+D_1+D_2+D_3 \quad (11)$$

Among them, A_3 is the third-level approximation component (low-frequency trend term), and to are the detail components (high-frequency terms) at each level. The detail components are combined into the noise term $N=D_1+D_2+D_3$, while the trend term is retained separately.

Figure 6 shows the wavelet decomposition results of the repaired sequence at monitoring point QCJ2-4. It can be seen from the figure that the trend component retains the overall variation pattern of the original sequence, reflecting the macroscopic evolution law of wall top settlement during foundation pit construction, while the noise component exhibits random fluctuation characteristics, mainly originating from construction disturbances, temperature changes, and monitoring errors. Through wavelet decomposition, multi-scale separation of the signal is achieved.

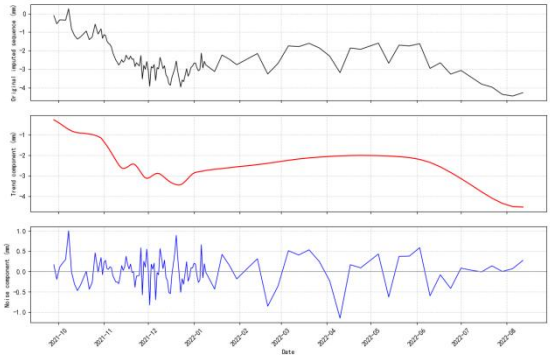

Figure 6 Wavelet Decomposition Result Plot of the Repaired Sequence at Monitoring Point QCJ2-4

3.4 GRU-ARMA Hybrid Prediction

After completing wavelet decomposition, the trend component and the noise component are obtained. Because the two components have different statistical characteristics, the GRU neural network and the autoregressive moving average (ARMA) model are used for prediction respectively, and then the prediction results are reconstructed to obtain the final deformation prediction value.

The trend component reflects the macroscopic evolution trend of wall top settlement and exhibits non-stationary and nonlinear characteristics, making it suitable for modeling with deep learning methods. In this paper, a two-layer stacked GRU network is constructed to predict the trend component, with its specific structure shown in Figure 7. The network consists of two GRU layers, each with 64 units. Dropout (rate 0.2) is added between layers to prevent overfitting. The output layer is a fully connected layer with an output dimension of 1. A rolling window approach is used to construct samples, with an input time step of 10 to predict the next single step. The training set and test set are split in an 8:2 ratio. The loss function is MSE, the optimizer is Adam, the number of training epochs is 100, and the batch size is 16.

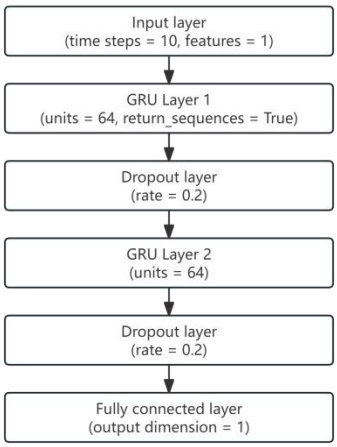

Figure 7 Structure Diagram of the GRU Network

The noise component N exhibits stationary random fluctuation characteristics and is fitted using the classical time series model ARMA. First, the stationarity of the noise series is verified by the ADF test. The test statistic is −6.1146,and the p-value is 0.0000($p<0.05$), so the null hypothesis is rejected and the series is stationary. Then, based on the ACF and PACF plots, combined with the AIC criterion, the optimal orders (p,q) are determined. After traversing p=0,...,4 and q=0,...4, the model with the minimum AIC is selected. Finally, the ARMA(3,2) model is determined as follows:

$$N_t=c+\phi_1 N_{t-1}+\phi_2 N_{t-2}+\phi_3 N_{t-3}+\varepsilon_t+\theta_1\varepsilon_{t-1}+\theta_2\varepsilon_{t-2} \quad (12)$$

Maximum likelihood estimation is used for parameter estimation, yielding the following parameter estimates:$c=1.438\times10^{-5}$, $\phi_1=1.537727$, $\phi_2=-0.778613$, $\phi_3=-0.011595$, $\theta_1=-1.998883$, $\theta_2=0.998883$.After model fitting, the residual white noise test (Ljung-Box test $p=0.5531>0.05$),indicates that the residuals have no autocorrelation, confirming the model's validity. The fitted model is then used for recursive prediction on the test set to obtain the predicted noise component $\hat{N}$。

The trend component prediction value obtained from the GRU model and the noise component prediction value obtained from the ARMA model are summed to obtain the final deformation prediction value $\hat{Y}=\hat{T}+\hat{N}$. Figure 8 shows the comparison curve between the actual deformation values on the test set and the prediction values of the proposed model. It can be seen from the figure that the predicted curve is in good agreement with the measured curve, accurately capturing both the overall trend and local fluctuations of the foundation pit deformation.

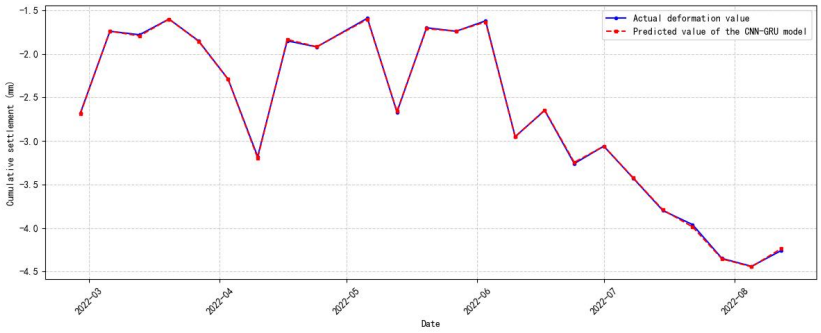

Figure 8 Comparison Chart of Prediction Curves

To further verify the superiority of the proposed model, it is compared with a single GRU model, a single ARMA model, and a GRU model without wavelet decomposition. RMSE, MAE, MAPE, and are used as evaluation metrics. The error metrics of each model on the test set are shown in Figure 9. It can be seen from Figure 9 that the proposed CNN-GRU hybrid model outperforms the comparison models significantly across all metrics, confirming the effectiveness of CNN imputation and wavelet decomposition in improving prediction performance.

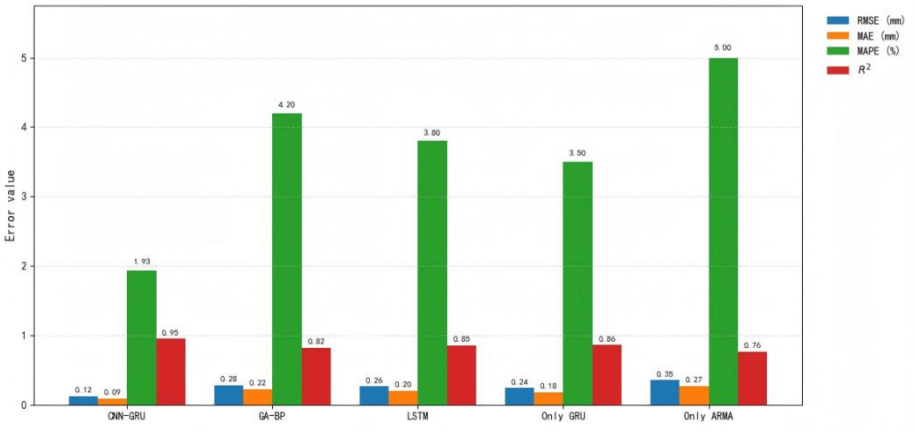

Figure 9 Comparison Chart of Prediction Errors of Different Models

3.5 Prediction Results

On the test set, the proposed CNN-GRU model achieves an RMSE of 0.12 mm, an MAE of 0.09 mm, a MAPE of 1.93%, and an R^2 of 0.95. In comparison, the single GRU model yields an RMSE of 0.24 mm, an MAE of 0.18 mm, a MAPE of 3.50%, and an R^2 of 0.86. The single ARMA model performs even worse, with an RMSE of 0.35 mm, an MAE of 0.27 mm, a MAPE of 5.00%, and an R^2. Compared with the single GRU model, the proposed model reduces RMSE and MAE by 50% and 50%, respectively; compared with the single ARMA model, it reduces them by 65% and 67%, respectively. The MAPE is reduced by 45% and 61%, while R^2 is increased by 10% and 25%, respectively. These results indicate that the combination of CNN-based missing data imputation and wavelet decomposition significantly improves the accuracy and stability of deformation prediction.

At the same time, compared with two commonly used neural networks, GA-BPand LSTM[12-18], the proposed model also shows clear advantages: GA-BP achieves an RMSE of 0.28 mm and a MAPE of 4.20%; LSTM achieves an RMSE of 0.26 mm and a MAPE of 3.80%. Compared with these two models, the proposed model reduces RMSE by 57% and 54%, respectively, and reduces MAPE by 54% and 49%, respectively, demonstrating the effectiveness and superiority of the proposed method under incomplete data conditions.

4 CONCLUSION

The CNN-GRU hybrid model proposed in this paper can effectively address the problem of missing monitoring data in subway foundation pits. In the prediction of vertical displacement at the wall top of No. 2 air vent at Terminal 3 Station of B Airport, the model achieves a MAPE of 1.93% and a coefficient of determination R^2 of 0.95. Compared with GA-BP, LSTM, single GRU, and ARMA models, the proposed model performs significantly better in terms of RMSE, MAE, MAPE, and other metrics, with no obvious prediction lag. It exhibits higher prediction accuracy and stronger engineering applicability, providing reliable support for foundation pit deformation prediction under incomplete data conditions.

COMPETING INTERESTS

The authors have no relevant financial or non-financial interests to disclose.

REFERENCES

[1] Liu Mengyang. Research on deformation prediction and active control of deep foundation pit excavation in subway stations. Huazhong University of Science and Technology, 2024. DOI: 10.27157/d.cnki.ghzku.2024.002630.

[2] Zhou Yi, Wang Zhangqiong, Zou Yuangeng, et al. Research on Prediction Method of Metro Foundation Pit Deformation Based on CNN-GRU Neural Network with Incomplete Data. Urban Rail Transit Research, 2025, 28(06): 32-36+53. DOI: 10.16037/j.1007-869x.20230612.

[3] Liu Cheng, Liu Yong, Rong Wenzhen, et al. Research on Prediction of Deformation of Foundation Pit Based on CNN-Attention-LSTM//Process Control Professional Committee of Chinese Society of Automation, Chinese Society of Automation. Proceedings of the 35th China Conference on Process Control. School of Automation and Information Engineering, Sichuan University of Light Chemical Technology; Sichuan Provincial Key Laboratory of Artificial Intelligence, 2024: 879. DOI: 10.26914/c.cnkihy.2024.020078.

[4] Yao Ronghan, Zhang Wensong, Jia Lei, et al. Settlement estimation model of buildings around subway foundation pit based on spatiotemporal characteristics and deep learning. Journal of Rock Mechanics and Engineering, 2025, 44(S1): 196-205.

[5] Gao Y, Xiao Z, Gong Z, et al. Spatiotemporal Deformation Prediction Model for Retaining Structures Integrating ConvGRU and Cross-Attention Mechanism. Buildings, 2025, 15(14): 2537.

[6] Cao Jing, Ding Wenyun, Zhao Dangshu, et al. Prediction of foundation pit deformation time series based on LSSVM-ARMA model. Rock and Soil Mechanics, 2014, 35(S2): 579-586. DOI: 10.16285/j.rsm.2014.s2.021.

[7] Bao Yanni, Shen Danyi, Shi Zhenming, et al. Application of ARMA model in the prediction of deformation of anchor foundation pits. Journal of Engineering Geology, 2021, 29(05): 1621-1631. DOI: 10.13544/j.cnki.jeg.2021-0527.

[8] Ma Zhigang, Yang Guolin, Liu Tao, et al. Wavelet GRU-ARMA Optimized InSAR Monitoring Settlement Prediction Method. Surveying and Mapping Bulletin, 2024, (12): 33-39. DOI: 10.13474/j.cnki.11-2246.2024.1206.

[9] Fang Qing, Chen Sheng, Liu Xuezhu, et al. Application of CNN-LSTM model based on variational mode decomposition in foundation pit deformation prediction. Mechanics and Practice, 2024, 46(05): 1015-1022.

[10] Tang Haoran, Hu Yao, Lei Huayang, et al. Prediction of surface displacement caused by foundation pit excavation based on deep learning. Transactions of the Chinese Society of Geotechnical Engineering, 2024, 46(S2): 236-241.

[11] Shi Xiangfeng, Wang Lifen, Shen Yang, et al. Research on Time Series Prediction of Ground Settlement in Foundation Pit Construction Based on GA-SVM. Construction Technology, 2017, 46(08): 16-19+31.

[12] Yang Zhongxiang, Zhang Liangyu, Lai Xingxiang, et al. Prediction of deformation of CNN-PSO-LSTM deep foundation pit considering spatial feature fusion. Shanxi Architecture, 2026, 52(07): 108-114+138. DOI: 10.13719/j.cnki.1009-6825.2026.07.021.

[13] Ma Zhigang. Extraction of surface settlement characteristics and optimization prediction of wavelet GRU-ARMA in mining area based on InSAR technology. Lanzhou Jiaotong University, 2024. DOI: 10.27205/d.cnki.gltec.2024.001540.

[14] Li Sihui, Liu Haiqing. Prediction of deformation of deep foundation pit based on LMD-PSO-LSSVM combined model. Journal of Underground Space and Engineering, 2018, 14(02): 483-489. DOI: 10.20174/j.juse.2018.02.026.

[15] Wang X, Qin Z, Bai X, et al. Research Progress of Machine Learning in Deep Foundation Pit Deformation Prediction. Buildings, 2025, 15(6): 852.

[16] Hu Dong, Zhang Xiaoping. Research on Prediction of Foundation Pit Deformation Based on Gray System Theory. Journal of Underground Space and Engineering, 2009, 5(01): 74-78+168.

[17] Han Feng. Research on combined prediction of foundation pit deformation under data filtering conditions. Geotechnical Engineering Technology, 2023, 37(04): 392-396.

[18] Liang Xiaolong, Qi Erheng, Wang Qiangkun, et al. Research on Combined Prediction Model of Foundation Pit Deformation Wavelet Denoising and BP Neural Network. Surveying, Mapping and Spatial Geographic Information, 2021, 44(01): 189-192+195.